

Measurement

Elsevier Editorial System(tm) for  
Manuscript Draft

Manuscript Number:

Title: MicroMED, design of a particle analyzer for Mars

Article Type: SI: MetroAeroSpace

Keywords: MicroMED; ExoMars 2020 mission, particle analyzer, Mars, dust.

Corresponding Author: Dr. Diego Scaccabarozzi, Ph.D. Mechanical engineering

Corresponding Author's Institution: Politecnico di Milano

First Author: Diego Scaccabarozzi, Ph.D. Mechanical engineering

Order of Authors: Diego Scaccabarozzi, Ph.D. Mechanical engineering;  
Bortolino Saggin; Christian Pagliara; Marianna Magni; Marco Tarabini;  
Francesca Esposito; Cesare Molfese; Fabio Cozzolino; Fausto Cortecchia;  
Gennady Dolnikov; Ilia Kuznetsov; Andrew Lyash; Alexander Zakharov

Abstract: Airborne dust monitoring is crucial to characterize Martian atmosphere' thermal structure, balance and dynamics. In order to achieve this objective, the MicroMED instrument has been selected to join the Dust Suite payload within the ExoMars 2020 mission. The particle analyzer is mainly developed to characterize the dust on Mars but, the instrument is suitable to be mounted on different landers or rovers thanks to the limited mass budget and size. In this study, design of the instrument has been reported as long as preliminary testing in representative environment of a mockup of the pumping system.

Suggested Reviewers: Alessandro Cozzani  
Engineering Services Section, ESA  
Alessandro.Cozzani@esa.int

Jens Romstedt  
ESTEC, ESA  
Jens.Romstedt@esa.int

Jorg Sekler  
Automation, University of Applied Sciences Northwestern Switzerland  
joerg.sekler@fhnw.ch

Piotr Orleański  
Centrum Badań Kosmicznych, Centrum Badań Kosmicznych  
porlean@cbk.waw.pl

Albert Haldemann  
ESTEC, ESA  
Albert.Haldemann@esa.int

**COVER LETTER**

**Subject:** Submission of “*MicroMED, design of a particle analyzer for Mars*” for the Special Issue 4th IEEE International Workshop on Metrology for Aerospace.

Dear Editor,

On the behalf of all the co-authors I am enclosing herewith the manuscript entitled “*MicroMED, design of a particle analyzer for Mars*”, extended version of the paper “Thermo-mechanical design of a particle analyzer for Mars”, published in 2017 at the 4<sup>th</sup> IEEE International Workshop on Metrology for Aerospace. The manuscript has been extended with optical layout design, description of the instrument pumping system and preliminary testing activity.

With the submission of this manuscript I would like to undertake that the above mentioned manuscript has not been published elsewhere, accepted for publication elsewhere or under editorial review for publication elsewhere; and that our Institute (Politecnico di Milano) representative is fully aware of this submission.

Correspondence should be addressed to:

Diego Scaccabarozzi  
Via G. Previati 1c, 23900 Lecco (LC)

[diego.scaccabarozzi@polimi.it](mailto:diego.scaccabarozzi@polimi.it)

telephone +39 (0)2 2399 88,

My best regards,

Ph.D. Diego Scaccabarozzi

# 1 MicroMED, design of a particle analyzer for Mars

2 Diego Scaccabarrozi<sup>1</sup>, Bortolino Saggin<sup>1</sup>, Christian Pagliara<sup>1</sup>, Marianna Magni<sup>1</sup>, Marco  
3 Tarabini<sup>1</sup>, Francesca Esposito<sup>2</sup>, Cesare Molfese<sup>2</sup>, Fabio Cozzolino<sup>2</sup>, Fausto Cortecchia<sup>2</sup>,  
4 Gennady Dolnikov<sup>3</sup>, Ilia Kuznetsov<sup>3</sup>, Andrew Lyash<sup>3</sup>, Alexander Zakharov<sup>3</sup>

5 1 Politecnico di Milano, Polo Territoriale di Lecco, Via g. Previati 1c, 23900 Lecco (Italy)

6 2 INAF - Osservatorio Astronomico di Capodimonte, Napoli, (Italy)

7 3 IKI RAN Space Research Institute of the Russian Academy of Sciences,

8 Moscow, Russia

9 \* corresponding author: [diego.scaccabarrozzi@polimi.it](mailto:diego.scaccabarrozzi@polimi.it)

## 10 Abstract

11 Airborne dust monitoring is crucial to characterize Martian atmosphere' thermal structure, balance  
12 and dynamics. In order to achieve this objective, the MicroMED instrument has been selected to  
13 join the Dust Suite payload within the ExoMars 2020 mission. The particle analyzer is mainly  
14 developed to characterize the dust on Mars but, the instrument is suitable to be mounted on different  
15 landers or rovers thanks to the limited mass budget and size. In this study, design of the instrument  
16 has been reported as long as preliminary testing in representative environment of a mockup of the  
17 pumping system.

## 18 Keywords

19 MicroMED; ExoMars 2020 mission, particle analyzer, Mars, dust.

## 20 Introduction

21 Airborne dust monitoring is very important for planetary climatology. Dust absorbs and scatter solar  
22 and thermal radiation, strongly modifying atmospheric thermal structure and balance. Moreover,  
23 blowing of sand and dust causes planetary surfaces shaping through the formation of sand dunes,

24 ripples, erosion of rocks and transport of soil particles. Martian atmosphere is characterized by  
25 regional and global dust storms that cause absorption of the incoming sunlight and consequently an  
26 intense atmospheric heating. Airborne dust is therefore a crucial climate component to be  
27 monitored. Beside dust and size distribution, knowledge of surface flux and granulometry would  
28 allow improvements of the existing Mars climate models. These are actually different observations  
29 of the dust haze from orbit but, the primary airborne dust size measurement (i.e. the one lifted from  
30 ground) has not been performed yet. This is the primary objective of MicroMED (Micro  
31 MEDUSA), miniaturized version of the instrument MEDUSA (Martian Environmental Dust  
32 Systematic Analyzer), developed for the Humboldt payload of the ExoMars mission [1].  
33 MicroMED would allow measurement of the abundance and size distribution of dust, not in the  
34 atmospheric column, but close to the surface, where dust is lifted, allowing monitoring of the dust  
35 injection into the atmosphere. The MicroMED has been selected to be mounted on the Dust Suite  
36 onboard the ExoMars 2020, suite of five sensors devoted to the study of Aeolian processes on Mars.  
37 Beside the MicroMED, Conductivity Sensor, Impact Sensor, Electric Probes and EM-sensor are  
38 present. The MicroMED is an optical particle counter that analyzes the light scattered from single  
39 dust particles to measure their size and abundance. A proper fluid-dynamic collector [2], including a  
40 pump [3] and a sampling head, allows the sampling of Martian atmosphere with embedded dust.  
41 Captured dust grains are detected by an optical system and then ejected into the atmosphere. The  
42 work undertaken for the preliminary design of the optical bench of the instrument is described in  
43 this paper as long as the instrument pumping system. In particular, finite element models of the  
44 instrument main components have been developed to allow mass fulfillment of the design budget  
45 and provide mechanical resistance against expected mechanical environment. Finally, testing  
46 activity of a mockup of the pumping system has been reported as proof of the proposed concept in  
47 low pressure environment.

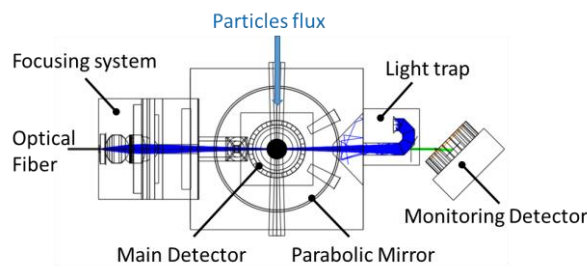
48 **1 MicroMED feasibility design**

49 *1.1 Instrument optical layout*

50 MicroMED instrument performs the measurement of the size of single dust grains and dust size  
51 distribution. A particle flux is created by a pumping system through a sampling volume, and laser  
52 beam light is focused in center of the sampling volume by means of an optical collimator. A  
53 collecting mirror conveys to a photodiode detector light scattered by particles flux. In order to reach  
54 the sampling volume with the laser, an optical fiber is used. This allows moving the diode laser  
55 source outside the sampling volume, and moreover, eases the instrument optical alignment. Thus,  
56 the optical system can be divided in three different sections:

- 57 • Diode laser source that feeds the optical fiber; and
- 58 • Focusing system of the light beam at the exit of the optical fiber, into a sampling volume;  
59 and
- 60 • Parabolic mirror, collecting and focusing the light, scattered by particles, onto the detector.

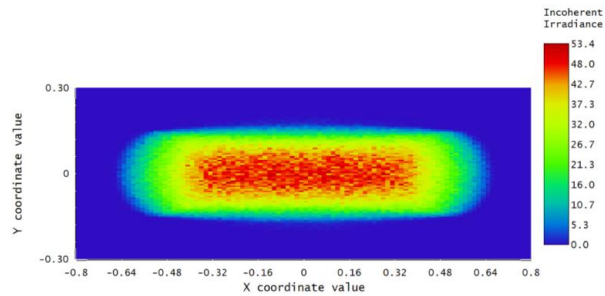
61 Moreover, in order to monitor laser diode performance that may change due to aging or exposure to  
62 radiation, an additional detector measures the signal derived from the light trap. Zemax NSC model  
63 of the instrument optical layout is shown in Figure 2.



64  
65 Figure 1 MicroMED optical layout (Zemax NSC model)  
66

67 The optical design is suitable for 780÷940 nm band, using fused silica glasses. Ray tracing analyses  
68 have been performed to derive the efficiency of the focusing system and obtain the optical density

69 in the sampling volume. For the optical density computation, conservative assumption has been  
70 made, i.e. minimum fiber output power was set to 128 mW (85% of laser power).



71

72 Figure 2 Beam spot onto a detector with size 1.6 mm x 600  $\mu\text{m}$ , in the center of the sample volume, with efficiency of  
73 88% ,  $10^6$  fired rays  
74

75 Figure 2 shows the shape of the spot obtained in a rectangular detector (1.6 mm x 600  $\mu\text{m}$ ), placed  
76 on the center of the sample volume, along the optical axis. More than the 88% of the rays emitted  
77 by the fiber are collected by the instrument detector, as preliminary validation of the optical design  
78 layout.

79 The design is still ongoing activity aiming to the definition of the opto-mechanical manufacturing  
80 tolerances, highlighting (if present) the influence of working temperature and pressure conditions.  
81 Moreover, analysis of the straight-light sensitivity of the MicroMED will be performed as well.

## 82 1.2 Thermo-mechanical design

### 83 1.2.1 Thermal analysis

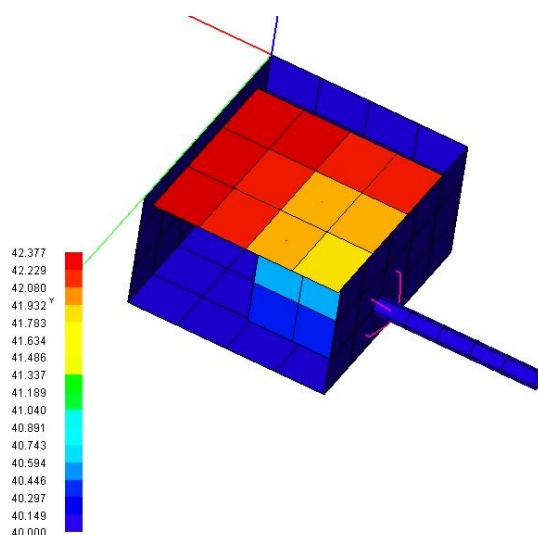
84 Instruments mounted on the Dust Complex suite are expected to work within controlled temperature  
85 range between -20  $^{\circ}\text{C}$  and 40  $^{\circ}\text{C}$  [4]. Storage temperature range is between -40  $^{\circ}\text{C}$  and 50  $^{\circ}\text{C}$ . The  
86 thermal requirements are not critical for the intended application. Anyway, a thermal model of the  
87 MicroMED envelope has been developed to assess if the highest interface temperature would lead  
88 to critical temperatures on the instrument internal components, electronics in particular.

89

Material	Thermal Conductivity [W/(mK)]	Emissivity
Al7075t6 (Alodine coating)	130	0.3
FR4/Cu electronics	36.6	1*

90

91 Model comprises the MicroMED envelope, the optical stage and the preliminary electronics board  
 92 layout. Materials and optical properties are summarized in Table 1. Temperature constraint at 40 °C  
 93 is set at the instrument base, whereas expected dissipated power is added to the instrument  
 94 electronic board. Thermal resistances have been computed at the joined interfaces. Steady state  
 95 analyses have been performed with radiative environment at 40 °C and 1 W dissipated power by  
 96 electronics. Computed temperature distribution is provided in Figure 3.



97

98 Figure 3 Temperature distribution computed with the hot case analysis. Measurement units are Celsius.  
 99

100 Temperature increase with respect the environment is limited to few degree Celsius. Thus, no  
 101 criticalities are foreseen both for the instrument and the electronics.

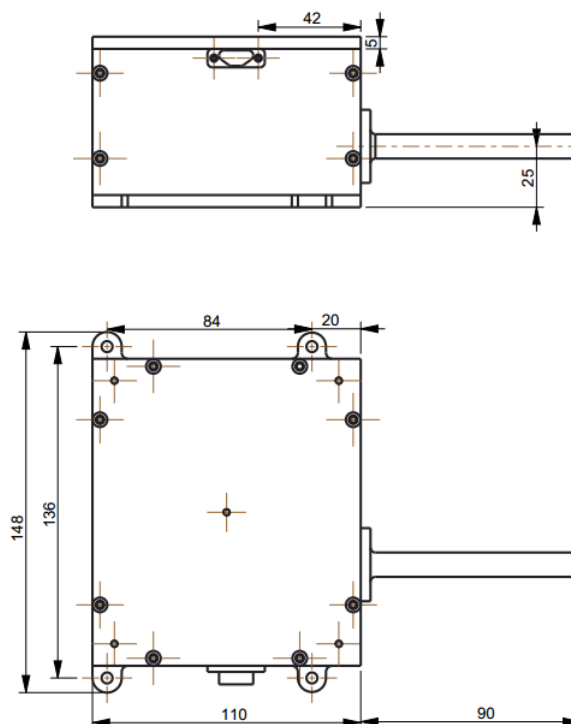
## 102 1.2.2 Mechanical requirements

103 Several requirements must be considered within the design of the MicroMED optical bench, mainly  
 104 coming from the accelerations during launch and landing operations [4]. Quasi-static acceleration

105 defined for the entry phase is somehow low, i.e. about  $100 \text{ m/s}^2$ . However, for the initial design  
106 phase, a quasi-static acceleration 10 times larger was considered. This was done on the basis of  
107 previous designed instruments [5-7], judged to be more conservative for the intended application.  
108 Mission dynamic requirement limits the resonance frequencies to be considered in the design phase  
109 at 150 Hz, value that allows a safety margin with respect to the strong sine excitation (ranging up to  
110 80 Hz) during the takeoff. Size of the instrument has been locked by preliminary interaction with  
111 the Roscosmos team which is manufacturing a structural model of the Exomars lander. Interface  
112 drawing is shown in Figure 4. Mass budget of the MicroMED is about 500g considering a maturity  
113 margin of 20%. The available mass for the optical bench (OB) and cover is 110g, including the  
114 supports of the main instrument components and fasteners.

### 115 1.2.3 Optical bench and cover optimization

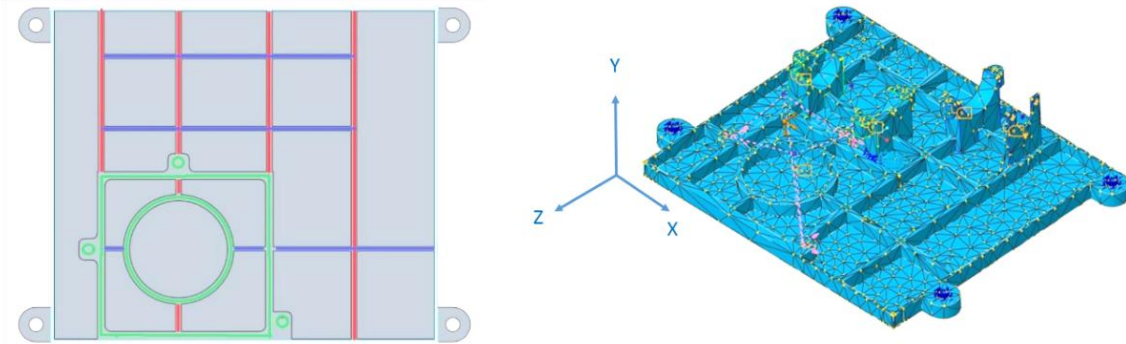
116 In order to satisfy the requirements described above, the design of the OB has been based on a  
117 ribbed geometry. Geometry and OB parameters are shown in Figure 5.  $w_{OBv}$  and  $w_{OBh}$  are widths of  
118 the vertical and horizontal ribs respectively, whereas  $th_{OB}$  is the OB thickness.





120

Figure 4 MicroMED interface drawings.



121

122 Figure 5 (Left) Configuration of the OB ribs from a top view; horizontal ribs (dark blue), vertical ribs (red), optical  
123 stage basement (green), diagonal rib (yellow), peripheral rib (light blue); (Right) OB meshed finite element model.  
124

125 The largest thickness of the OB has been set to 5 mm. The ribs configuration assures both for  
126 stiffening the OB and for holding the MicroMED subassemblies, as shown in Fig. 3. Al 7075 alloy  
127 has been selected for the OB development. Mechanical properties accounted in the model are 71700  
128 MPa (elastic modulus), 0.33 (Poisson ratio) and 2810 kg/m<sup>3</sup> (density).

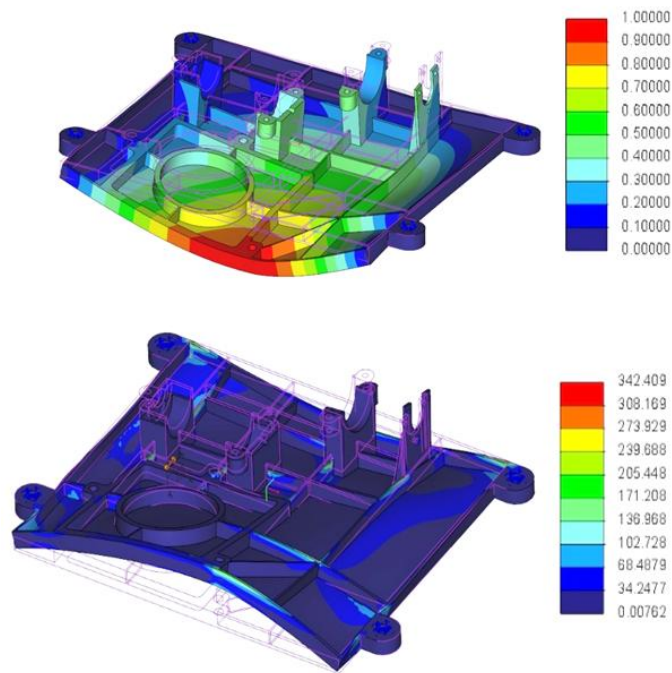
129 Optimization was performed minimizing the OB mass and considering as constraints, either first  
130 natural frequency larger than 150 Hz and safety margin of 1.5 with respect the tensile yield strength  
131 (503 MPa) with quasi-static analyses.

132 The Finite Element (FE) model comprises 6676 solid tetrahedrons elements and 2246 nodes. OB  
133 mesh is shown in Figure 5. Table 2 summarizes range of variability of the OB parameters and  
134 optimal results.

135

TABLE 2: OB OPTIMIZATION PARAMETERS AND RESULTS.

Parameter	Minimum [mm]	Maximum [mm]	Optimal [mm]
$w_{OBv}$	0.5	2	0.56
$w_{OBh}$	0.5	2	0.95
$th_{OB}$	0.1	0.4	0.21



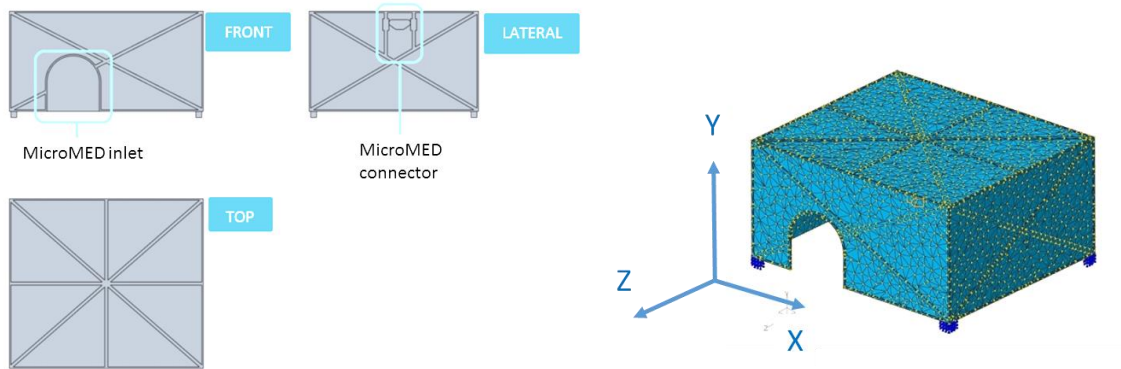
136

137 Figure 6 First mode of vibration (top) and Von Mises stress for static analysis (bottom) with optimized OB. Stress units  
 138 are MPa.

139 The instrument components are accounted as lumped masses and the OB is connected to the ground  
 140 with the interface feet at the holes surfaces. Optimization led to OB mass of about 38g. Resulting  
 141 first mode of vibration (150 Hz) and VM stress along Z direction are shown in Figure 6.

142 Structural requirements for the cover design are the same of MicroMED OB previously defined.  
 143 One main difference is that the first acceptable resonance of the structure was set to 250 Hz. This  
 144 was defined in order to avoid coupling with the OB modes on which the cover is mounted. Another  
 145 difference regards the mass budget. The available mass limit is 55g. Keeping into account the  
 146 geometry of the OB and size constraints, cover was defined as an empty rectangular box (65 mm  
 147 height) with 110 x 124 mm base.  $w_{Cf}$ ,  $w_{Cl}$ ,  $w_{Ct}$  are widths of the front, lateral and bottom surfaces,  
 148 respectively. Similarly,  $th_{Cf}$ ,  $th_{Cl}$  and  $th_{Ct}$  are cover' thicknesses of the front, lateral and bottom  
 149 surfaces. The largest thickness of the cover was set to 2 mm. Two apertures were added to the case,  
 150 to allow mounting of the cover without interference with the OB optical stage. Cover ribs and cover  
 151 FE model are shown in Figure 7. Mesh comprises 18445 solid tetrahedrons elements and 6059

152 nodes. The geometry was constrained on four L profiles in the internal edges of the cover to serve  
 153 as mountings with the cover. Cover material is aluminum alloy Al7075T6.



154

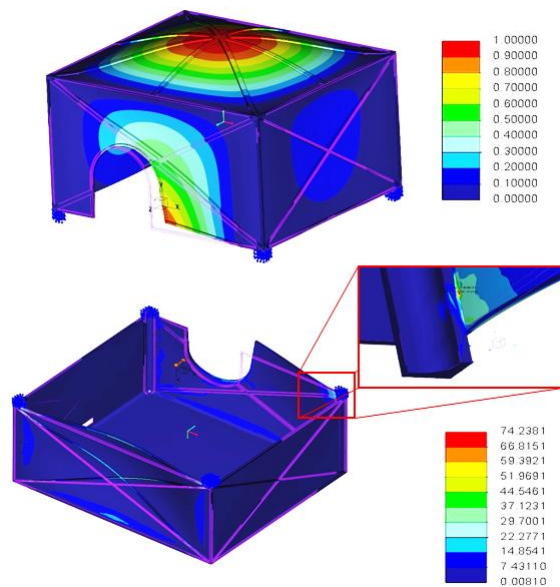
155 Figure 7 (Left) Configuration of the cover ribs FE model mesh and reference system; (right) cover meshed finite  
 156 element model.

157

TABLE 3 COVER OPTIMIZATION PARAMETERS AND RESULTS.

Parameter	Minimum [mm]	Maximum [mm]	Optimal [mm]
$w_{Cf}$	0.5	3	1.93
$w_{Ct}$	0.5	3	0.66
$w_{Cl}$	0.5	3	2.55
$th_{Cf}$	0.1	1	0.2
$th_{Cl}$	0.1	1	0.2
$th_{Ct}$	0.1	1	0.2

158



159

160 Figure 8 First mode of vibration (top) and Von Mises stress for static analysis (bottom) with optimized cover. Stress  
 161 units are MPa.

162 Optimization was performed minimizing the cover mass and considering results of the modal and  
163 static analyses as constraints. Table 3 provides parameters range and optimization results. Cover  
164 mass after minimization was found to be 39.4g. Figure 8 shows results of the FE modal (first mode  
165 at 250 Hz) and static analysis (loading case along Z direction).

166 Summarizing the results of the feasibility design it can be noticed that horizontal ribs are the ones  
167 most affecting the mass reduction and modal behavior of the OB, as demonstrated by the first mode  
168 of vibration shown in Figure 6, where bending of the OB is involving the stiffness of the horizontal  
169 ribs.

170 A similar result was found for the cover; lateral and front ribs are the ones most affecting the modes  
171 of vibration of the cover.

172 The overall mass is about 78g, providing mass saving of 30% with respect to the mass budget,  
173 validating the feasibility design.

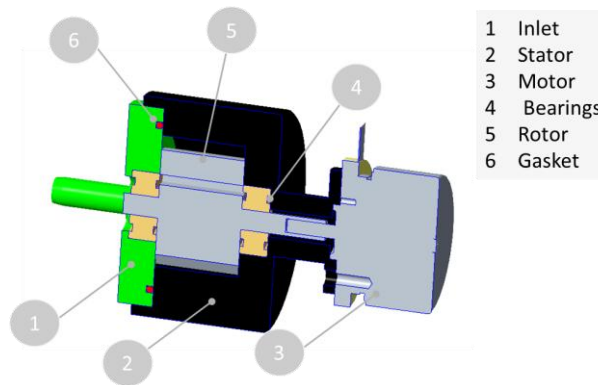
#### 174 1.2.4 Pumping system

175 In order to achieve the dust flux through the optical head, pumping system has been designed.  
176 Gardner Denver Thomas G 6/04 EB was used as a reference for the design of the pump for Mars.  
177 Pump mass budget is constrained to 30g. The geometry and the size of the compression chamber,  
178 inlet and outlet ports maintained the same geometry of the commercial pump, but only space  
179 qualified materials have been used. Thus, the commercial pump underwent to a process of reverse  
180 engineering that allowed identifying the criticalities for space usage. These were mainly related to  
181 the outgassing of the materials, resistance against the expected mechanical loading and compliance  
182 with the thermal environment. Main changes applied to the pump scheme are shown in Figure 9 and  
183 are summarized hereafter:

- 184 • Pump rotor and shaft (5) are made of Aluminum alloy (Al7075T6) instead of the  
185 combination of steel and plastic used in the commercial pump; and

- 186 • Stator (2) is made in aluminum alloy as well; inner surface of the compression chamber is  
187 anodized to limit friction between stator and rotor and avoid soldering between stator and  
188 rotor during the lunch (due to high loading); and
- 189 • Vanes and palettes are made of Vespel SP1, which limit outgassing and provides self-  
190 lubrication; and
- 191 • Two radial bearings (4) are mounted in back to back configuration and preloaded to take out  
192 the quasi-static loading at the landing, both in axial and radial directions, to avoid the  
193 hammering due to vibration at launch, and to assure proper working during the pump  
194 activity; in the commercial pump only one radial ball bearing was present to accomplish the  
195 latter task.

196 Selected materials would provide the sealing of the pumping chamber at every temperature since CT  
197 allows to recover the CTE difference between the rotor, vanes, sealing elements and aluminum pump  
198 case (1).



199

200

Figure 9 MicroMED pump design concept.

201 The final configuration is based on a Maxon EC 20 brushless motor, not qualified but similar model  
202 has been used in previous mission driller. Motor mass is 22 g mass without control electronics. The  
203 motor provides about 31 Nmm stall torque and 8.3 Nmm torque in continuous working and  
204 maximum continuous power provided by the motor 5W.

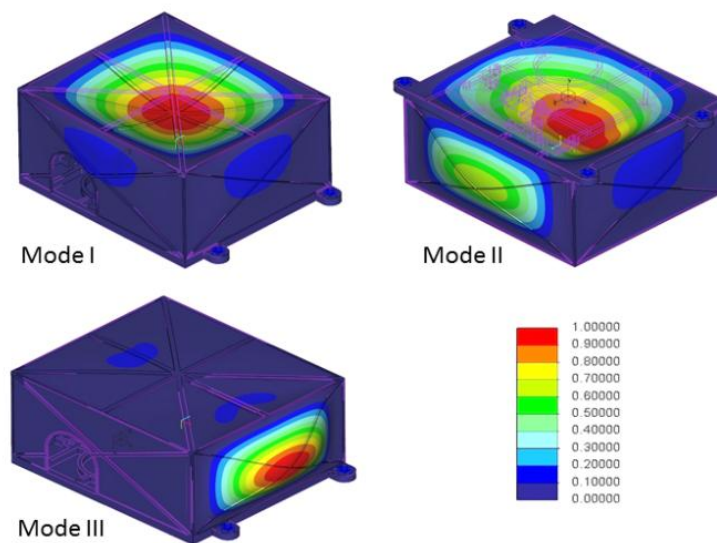
205 1.2.5 MicroMED envelope detailed design

206 Review of fundamental geometries and dimensions of the MicroMED OB and cover was performed  
 207 in order to overcome technological limits related to the ribs manufacturing. Ribs layout of the  
 208 MicroMED optimal model is kept as reference but the parameters were modified as show in Table 4.  
 209 Change of the ribs led to mass increase of about 24% and 7.5% for the OB and cover, respectively. A  
 210 FE model of the instrument was made. Meshed geometry comprises 68913 solid tetrahedrons  
 211 elements and 22253 nodes.

212 TABLE 4 MICROMED DETAILED DESIGN.

Parameter	Detailed design value [mm]
$w_{OBv}, w_{OBh}$	2
$th_{OB}$	0.2
$th_{Cf}, th_{Cl}, th_{Ci}$	0.2
$w_{Cf}, w_{Cl}$	2
$w_{Ci}$	3

213  
 214 Modal analyses were performed on the detailed instrument model. Results are shown in Figure 10.  
 215 First three modes of vibration are located on the MicroMED cover at 260, 325 and 388 Hz,  
 216 respectively.



217  
 218 Figure 10 Results of modal analyses, with detailed MicroMED model.

219 Obtained stiffening is due to the increase of the ribs' width that compensate the compliance of the  
220 cover constraint, connected to the OB rather than to ground (as for optimization). Quasi static  
221 analyses were performed as well. Positive MOSs (Margin Of Safety) were obtained, thus validating  
222 the performed mechanical design for the detailed model as well.

## 223 **2 Flow rate testing in low pressure condition**

224 Testing of the pumping system in low pressure condition is required to verify the pumping  
225 performances in working condition. The pump characterization is of primary interest, because the  
226 generated flow rate affects the instrument measurement range, i.e. particle size and collecting  
227 efficiency. Preliminary fluid dynamic analyses evidenced flow rate requirement between 1.5 and 1.2  
228 L/min with 3 mbar pressure difference to be overcome by the pumping system, with Martian  
229 atmosphere temperature between 150 and 300 K. The 3 mbar pressure difference has been identified  
230 as the best working condition to sample the particles ranging between 0.5 and 20  $\mu\text{m}$ .

231 However, the measurement of the flow rate in low pressure condition is not an easy task since the  
232 commercially available sensors are not directly applicable to low pressure environment and must be  
233 calibrated. Thus, we designed a setup based on a bellow which acts as collecting volume of the flux  
234 at the pump outlet. Details of the setup design and validation are described in authors' manuscript  
235 under review. Sketch of the measurement setup is shown in Figure 11. A differential pressure sensor  
236 is mounted as well to measure the pressure difference change during the bellow displacement  
237 (measured by means of laser transducer, ILD 1400 Micro-Optronic, 100 mm range). Pressure in the  
238 chamber was monitored by means of vacuum gauge (Varian PCG-750). Testing was performed with  
239 the commercial pump Gardner Denver Thomas G 6/04 EB at ambient temperature and 10 mbar  
240 pressure condition. Figure 12 shows measurement results.

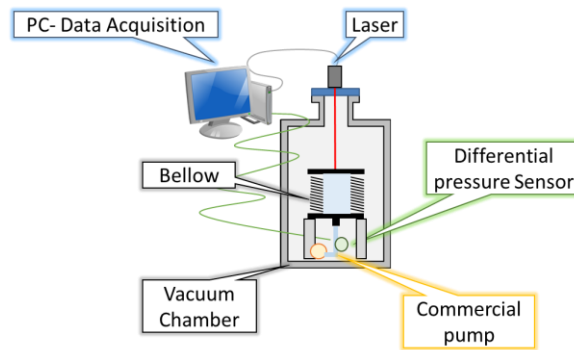


Figure 11 Scheme of the flow rate measurement setup.

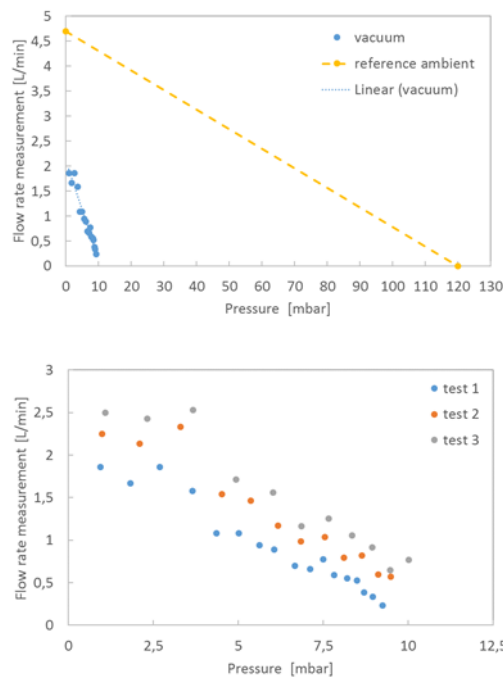


Figure 12 Flow rate measurement, commercial pump (@10mbar, ambient temperature): (Top) comparison between measured flow rate in low pressure condition and reference curve and (bottom) repeatability of the measured flow rate in low pressure condition.

The main result is that pump performances clearly worsen in low pressure condition. Measured performance provides lower flow rate and maximum working pressure is limited to 10 mbar. Repeatability assessment evidenced similar trends of the measured flow rate. Comparison of subsequent tests (number from 1 to 3) shows average increase of the flow rate. This has been endorsed to change in gas temperature (due to heating in the compression chamber) that would lead to increase of the volumetric flow rate. Anyway, the measured performance is compatible with the design requirement, validating the usage of the identified pumping system for the MicroMED development.





### 256 3 Conclusions

257 The main result of this work is the assessment of the feasibility of the MicroMED instrument, a dust  
258 analyzer for Mars. The feasibility study was carried-out by means of finite element modelling,  
259 developing different FE models of the instrument' optical bench and cover. Modal and quasi-static  
260 stress analyses were performed to verify the dynamic behavior and the mechanical resistance of the  
261 main components under the design loads. The instrument geometry was optimized with the goal of  
262 minimizing the instrument overall mass. Optimization led to a mass saving of 30 % with respect to  
263 the allocated mass and the fulfilling of the design requirements about mass margins.

264 Beside the optimization study, a detail design of the MicroMED was performed changing ribs'  
265 dimension to values set to manufacturing limits. Modal and mechanical analyses were performed as  
266 well, comparing the results with those deriving from the optimization. An increase of the natural  
267 frequencies (lowest natural frequency is about 260 Hz) and of the overall mass was found. The latter  
268 is 1.5 % larger than the allowed maximum one (considering also the mass budget to be located for  
269 the supports of the instrument components). Thus, being the obtained overall mass within the  
270 tolerated deviation from the design requirement, the feasibility design of the MicroMED was  
271 successfully demonstrated.

272 Pumping system has been re-designed starting from a commercial pump preliminary selected to be  
273 used in an instrument breadboard. The re-design allows withstanding the expected mechanical  
274 loading and operate in low pressure condition. This was preliminary validated by testing of the  
275 commercial pump in representative environment. Additional testing is planned to validate the new  
276 pump design in low pressure and within expected temperature working conditions.

277

278

279 **Figure Captions**

280 Figure 1 MicroMED optical layout (Zemax NSC model)

281

282 Figure 2 Beam spot onto a detector with size 1.6 mm x 600  $\mu\text{m}$ , in the center of the sample volume,  
283 with efficiency of 88% , 106 fired rays

284

285 Figure 3 Temperature distribution computed with the hot case analysis. Measurement units are  
286 Celsius.

287

288 Figure 4 MicroMED interface drawings.

289

290 Figure 5 (Left) Configuration of the OB ribs from a top view; horizontal ribs (dark blue), vertical  
291 ribs (red), optical stage basement (green), diagonal rib (yellow), peripheral rib (light blue); (Right)  
292 OB meshed finite element model.

293

294 Figure 6 First mode of vibration (top) and Von Mises stress for static analysis (bottom) with  
295 optimized OB. Stress units are MPa.

296

297 Figure 7 (Left) Configuration of the cover ribs FE model mesh and reference system; (right) cover  
298 meshed finite element model.

299

300 Figure 8 First mode of vibration (top) and Von Mises stress for static analysis (bottom) with  
301 optimized cover. Stress units are MPa.

302

303 Figure 9 MicroMED pump design concept.

304

305 Figure 10 Results of modal analyses, with detailed MicroMED model.

306

307 Figure 11 Scheme of the flow rate measurement setup.

308

309 Figure 12 Flow rate measurement, commercial pump (@10mbar, ambient temperature): (Top)

310 comparison between measured flow rate in low pressure condition and reference curve and (bottom)

311 repeatability of the measured flow rate in low pressure condition condition.

312

313 **Table Captions**

314 Table 1 Materials and optical properties

315

316 Table 2 OB optimization parameters and results

317

318 Table 3 Cover optimization parameters and results

319

320 Table 4 MICROMED detailed design

321

322 **References**

323 [1] Colangeli, L., Lopez-Moreno, J. J., Nørnberg, P., Della Corte, V., Esposito, F., Epifani, E. M., ...  
324 & Rotundi, A. , MEDUSA: The ExoMars experiment for in-situ monitoring of dust and water  
325 vapour, *Planet Space Sci*, 57 (2009), 1043-1049. DOI: 10.1016/j.pss.2008.07.013.

326

327 [2] Messa, G. V., Malavasi, S., Scaccabarozzi, D., Saggin, B., Tarabini, M., Esposito, F., &  
328 Molfese, C. , Preliminary design of the inlet duct of a dust analyzer for Mars, *IEEE Metrology for*  
329 *Aerospace*, (2016), pp. 604-608. DOI: 10.1109/MetroAeroSpace.2016.7573285.

330

331 [3] Scaccabarozzi, D., Tarabini, M., Almasio, L., Saggin, B., Esposito, F., & Cozzolino, F.,  
332 Characterization of a pumping system in Martian-like environment, (2016), *IEEE Metrology for*  
333 *Aerospace*, (2014), 150-154. DOI: 10.1109/MetroAeroSpace.2014.6865911.

334

335 [4] Russian Academy of Sciences, Space Research Institute (IKI), 'ExoMars 2018 Surface  
336 Platform Experiment Proposal Information Package', (2015).

337

338 [5] Saggin, B., Tarabini, M., & Scaccabarozzi, D., Infrared optical element mounting techniques for  
339 wide temperature ranges, (2010), *Appl Optics*, 49, 542-548. DOI: 10.1364/AO.49.000542.

340

341 [6] Scaccabarozzi, D., Saggin, B., & Alberti, E., Design and testing of a roto-translational shutter  
342 mechanism for planetary operation, *Acta Astronautica*, 93 (2014), 207-216. DOI:  
343 10.1016/j.actaastro.2013.07.006

344

345 [7] Shatalina, I., Saggin, B., Scaccabarozzi, D., Panzeri, R., Bellucci, G., MicroMIMA FTS:  
346 design of spectrometer for Mars atmosphere investigation, Remote Sensing of Clouds and the  
347 Atmosphere XVIII, 2013, DOI: 10.1117/12.2028644.

348